

Non-heat-stressed Method to Isolate Hepatic Stellate Cells From Highly Steatotic Tumor-bearing Liver Using CD49a

メタデータ	言語: English 出版者: Elsevier 公開日: 2022-10-07 キーワード (Ja): 肝がん, 高度脂肪肝, 肝星細胞 キーワード (En): 作成者: 程, 禎, 山岸, 良多, 野中, 允幾, 松原(佐藤), 三佐子, 河田, 則文, 大谷, 直子 メールアドレス: 所属: Osaka Metropolitan University, Osaka Metropolitan University, Osaka City University, Osaka Metropolitan University, Osaka Metropolitan University, Osaka Metropolitan University, Japan Agency for Medical Research and Development
URL	https://ocu-omu.repo.nii.ac.jp/records/2019707

Non-heat-stressed Method to Isolate Hepatic Stellate Cells From Highly Steatotic Tumor-bearing Liver Using CD49a

Yi Cheng, Ryota Yamagishi, Yoshiaki Nonaka, Misako Sato-Matsubara, Norifumi Kawada, Naoko Ohtani

Citation	Cellular and Molecular Gastroenterology and Hepatology. 14(4); 964-966.e9
Version of record	2022-09-19
Type	Journal Article
Textversion	Publisher
Highlights	◇肝がんの特性を理解するには、様々な状態の肝臓から肝星細胞を効率良く単離してがん微小環境における肝星細胞の性質を解析する必要がある。 ◇脂肪肝の場合、狙った肝星細胞の単離が難しく、また熱ストレスの影響で正確な遺伝子情報の解析ができなかったが、特定の肝星細胞をより精密に単離する方法を開発した。
Rights	© 2022 The Authors. Published by Elsevier Inc. This work is licensed under a Creative Commons Attribution-NonCommercial-NoDerivatives 4.0 International License. https://creativecommons.org/licenses/by-nc-nd/4.0/deed.en
DOI	10.1016/j.jcmgh.2022.07.006

Self-Archiving by Author(s)
Placed on: Osaka City University

概要

研究グループは、肝がんを伴う高度脂肪肝から肝星細胞を単離する方法を開発しました。本研究成果により、これまで解析されていなかったがん微小環境における肝星細胞の1細胞レベルの性質変化が明らかになり、がん予防や治療につながるものが期待されます。

がんの組織はがん細胞そのものだけでなく、肝星細胞など様々な種類の細胞種が集まってがん微小環境を構成しています。本研究グループが以前明らかにしたように、肝がんでは腫瘍部に存在する肝星細胞から分泌される因子が抗腫瘍免疫を抑制し、肝がんを進展させます。そのため、肝がんの特性を理解するには、様々な状態の肝臓から肝星細胞を効率良く単離して、微小環境における肝星細胞の性質を解析する必要があります。

近年、シングルセル RNA シーケンス解析の手法が発達し、1細胞レベルでの細胞の性質解析が可能となりました。これまでマウスの正常肝から肝星細胞を単離する方法は報告されていましたが、内臓脂肪を多く蓄積した肥満マウスの脂肪肝や、脂肪肝を素地とする腫瘍に存在する肝星細胞を高純度かつ高効率に単離する方法は開発されていませんでした。また、細胞単離時に使用する酵素処理を37度で実施すると、熱ストレス関連遺伝子が有意に発現上昇し、アーティファクトとなることも報告されていました。

そこで本研究グループは、内臓脂肪を多く蓄積した脂肪肝の腫瘍部から、熱ストレス関連アーティファクトを極力抑えた6度という低温で酵素処理し、かつ、密度勾配遠心分離法と肝星細胞の細胞表面分子 CD49a を用いたセルソーティングを組み合わせた方法により、高純度に効率よく肝星細胞を単離する方法の開発に成功しました。(図1)

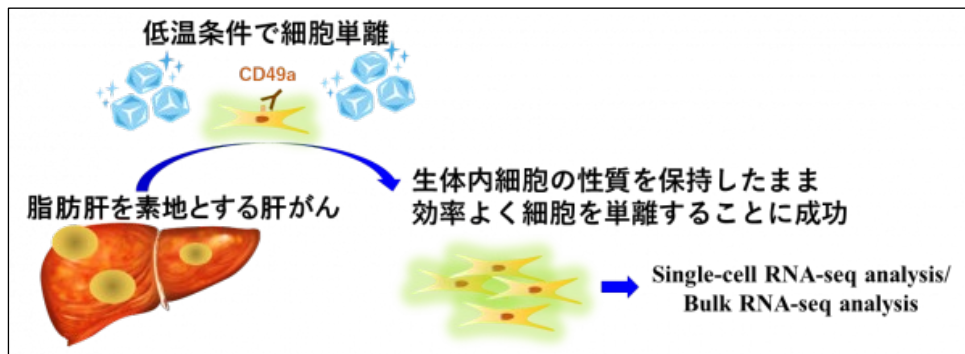


図1. マウスとヒトの肝癌組織から低温条件(6°C)で高純度の肝星細胞を単離することに成功

Description

<研究の背景>

がんの進展にはがん微小環境の変化が重要ですが、肝がんの場合、腫瘍部に存在する肝星細胞から分泌される因子が抗腫瘍免疫を抑制し、肝がんを進展させることを本

研究グループは先行研究で報告し、肝星細胞の重要性を示してきました。(Yoshimoto et al. Nature 2013, Loo et al. Cancer Discovery 2017, Yamagishi et al. Science Immunology, 2022)。近年、シングルセル RNA シーケンス解析の手法が発達し、1 細胞レベルでの細胞の性質解析が可能となっています。したがって、脂肪肝を素地とする腫瘍部を含め様々な状態の肝臓から、肝星細胞を単離する方法を開発し、微小環境における肝星細胞の性質を解析する必要があります。

これまで、マウスの正常肝から肝星細胞を単離する方法は報告されていましたが、内臓脂肪を多く蓄積した肥満マウスの脂肪肝や、脂肪肝にともなう肝がん部からの肝星細胞の高効率単離法は開発されていませんでした。また、細胞単離時に使用する酵素処理を 37 度で実施すると、熱ストレス関連遺伝子が有意に発現上昇し、アーティファクトとなることも報告されていました。そのため、熱ストレス関連アーティファクトを極力抑える手法が求められていました。

<研究の内容>

脂肪肝を呈する肥満マウスでは内臓脂肪が高度に蓄積しており、下大静脈が内臓脂肪により、非常に見えにくいいため、正常マウス肝から肝星細胞を単離する場合に、還流に使用する下大静脈からの還流ルートの確保が非常に困難です。そこで、本研究グループは高度肥満マウスでも確実に還流ルートを確保できる門脈を介するルートを用いることで、この点を克服しました。また、熱ストレス関連遺伝子が有意に発現上昇する 37 度での酵素処理はアーティファクトの遺伝子発現を含んでしまう危険性があるため、近年、低温の 6 度で細胞単離したシングルセル RNA シーケンス解析がいくつかの論文で推奨されています。この点については、使用するコラゲナーゼなどの組織の分解酵素は、肝臓においては 運よく 6 度の条件でも機能しました。ただ、肝腫瘍部においては、類洞構造が崩れているため、還流操作では、組織に酵素液が行き渡らないため、組織をハサミでミンスすることで、酵素を反応させました。

次に、肝星細胞を多く含む細胞分画を得るため、様々な密度勾配液の濃度を変えて密度勾配遠心分離を行いました。その結果、ナイコデントを用いた密度勾配液が 13% の濃度で遠心分離を行った場合に、肝星細胞が最も多い分画となりました。この分画を用いて、免疫細胞と血管内皮細胞をその表面分子を利用して除いた細胞集団において、シングルセル RNA seq 解析を行いました。しかし、この方法では、免疫細胞と血管内皮細胞は排除できているものの、肝実質細胞や肝がん細胞が混入していました。そこで、シングルセル解析の結果から、肝星細胞に特異的な細胞表面分子、CD49a を同定し、免疫細胞、血管内皮細胞を除いた細胞集団の中から、CD49a 陽性の細胞を、セルソーティングの手法で単離することで、高純度に肝星細胞を単離することに成功しました。

	<p>この方法で、別の遺伝的肥満マウスモデルの肝星細胞や、ヒトの肝がん組織における肝星細胞も単離することが可能となりました。</p> <p><今後の展開></p> <p>今後この手法を用いて、様々な脂肪肝モデルマウスやヒトの肝腫瘍組織から肝星細胞を高効率に単離することが可能となり、がん部や正常の肝組織特異的な肝星細胞の性質が明らかになることが期待されます。それにより、これまで十分に解析されていなかったがん微小環境における肝星細胞の1細胞レベルの性質変化が明らかになり、将来的には、がん予防や治療につながる分子標的の同定につながることを期待されます。</p>
<p>Funding</p>	<p>日本医療研究開発機構（AMED）の革新的先端研究開発支援事業(AMED CREST)「微生物叢と宿主の相互作用・共生の理解と、それに基づく疾患発症のメカニズム解明」領域における研究開発課題「腸肝軸を介した腸内細菌叢が関わる肝疾患発症メカニズムの解明とその制御（研究開発代表者：大谷直子） JP20gm1010009」、</p> <p>AMED 革新的がん医療実用化研究事業「がん微小環境における細胞間ネットワークの制御による新規がん予防・治療法の開発（研究開発代表者：大谷直子） P19ck0106260」、</p> <p>公益財団法人高松宮妃癌研究基金（研究代表者：大谷直子）</p> <p>公益財団法人武田科学振興財団（研究代表者：大谷直子）</p> <p>公益財団法人ヤクルト・バイオサイエンス研究財団（研究代表者：大谷直子）</p>

‘肝がんを伴う高度脂肪肝から肝星細胞を単離する方法を開発～1細胞レベルでの細胞の性質解析が可能に～’
大阪公立大学. https://www.omu.ac.jp/info/research_news/entry-02029.html. (参照 2022-09-12)

RESEARCH LETTER

Non-heat-stressed Method to Isolate Hepatic Stellate Cells From Highly Steatotic Tumor-bearing Liver Using CD49a

The number of patients with non-viral, nonalcoholic steatohepatitis-associated liver cancer has been increasing with the prevalence of obesity. Increasing evidence shows that the tumor microenvironment (TME) is crucial for tumor progression. We previously showed that hepatic stellate cells (HSCs) play key roles in tumorigenic TME of obesity-associated hepatocellular carcinoma (HCC) by secreting senescence-associated secretory factors that suppress anti-tumor immunity.¹⁻³ Recent advances in single-cell RNA-sequencing (scRNA-seq) techniques have enabled the characterization of different cell types in various tissues. Therefore, development of a refined method to characterize HSCs in TME under various conditions is necessary to understand their role in HCC progression.

Isolation of HSCs from normal liver via perfusion from the inferior vena cava (IVC) using a retrograde approach has been reported.⁴ However, this method is not applicable to highly steatotic liver or steatohepatic tumor tissues in obese mice as the accumulation of adipose tissue in obese mice hinders IVC visualization, thereby making cannulation via IVC difficult. Therefore, we attempted HSC isolation through the portal vein (PV), which is clearly visible under all conditions. We aimed to develop a method to isolate HSCs at a low temperature (6 °C) to minimize over digestion by enzymes and heat-associated stress after dissociation (at 37 °C), which reportedly induce genes such as *Fos* and *Jun*.⁵ Furthermore, we identified a cell

surface marker abundantly expressed in HSCs, which is useful for HSC cell sorting from murine and human liver tumor tissues.

In this proposed protocol, cannulation via PV and digestion using ice-cold enzymatic solution (Figure 1, A–B) are important steps for successful HSC isolation. We confirmed that the ice-cold enzyme solutions (pronase E, collagenase, and DNase I) retained enzymatic activity at 6 °C. The HSCs were concentrated using Nycodenz gradient medium (Supplementary Figure 1, A–D). The expression of *Lrat*, a marker for HSCs, revealed maximum HSC fraction in 13% Nycodenz gradient medium (Supplementary Figure 1, A). Pronase E was used to destruct hepatocytes,⁶ and almost no live hepatocyte contamination was confirmed. In contrast, increased contamination with macrophages (*Clec4f* expressing cells) and liver sinusoidal endothelial cells (LSECs, *Stab2* expressing cells) was observed at higher concentrations of Nycodenz (Supplementary Figure 1, B–C). Therefore, we decided to use 13% Nycodenz gradient medium for the subsequent experiments including flow cytometry and cell sorting.

To screen HSC-specific cell surface markers, we sorted CD31⁺/CD45⁻ cells from the HSC-rich 13% Nycodenz fraction and performed scRNA-seq using the CD31⁺/CD45⁻ fraction, excluding LSECs and immune cells (Figure 1, C). In the t-distributed stochastic neighbor embedding (t-SNE) analysis (Figure 1, D), clusters 0, 1, 2, and 6 predominantly expressed *Lrat*, indicating that they were HSC fractions (Figure 1, E). However, the other clusters consisted mainly of hepatocytes and HCC cells (*Hnf4a*-expressing cells), but almost no cholangiocytes (*Krt19*-expressing cells) were observed (Supplementary Figure 2, A). Among the top 50 genes expressed in the HSC clusters, we focused on 11 genes encoding cell surface molecules expressed in HSCs obtained from the livers of normal diet (ND)-fed mice (clusters 0 and 6 in Figure 1, E) and in those obtained from non-tumor (NT)

(cluster 1) and tumor (T) (cluster 2) segments of high-fat diet (HFD)-fed mice (Supplementary Figure 2, B). All 3 segments comprised *Itga1* (encoding integrin alpha1, CD49a in CD classification), indicating that *Itga1* was the most commonly expressed surface molecule gene. Moreover, *Itga1* distribution highly overlapped with *Lrat* distribution in the HSC clusters (Figure 1, F), indicating that *Itga1* (CD49a) could be an excellent HSC cell surface marker in the livers of both ND-fed and HFD-induced HCC-bearing mice. Therefore, we sorted the CD49a-high cell population among CD31⁺/CD45⁻ cells (Supplementary Figure 1, E; Figure 1, G) and conducted scRNA-seq analysis. *Itga1* (CD49a) was confirmed as a promising HSC marker comparable to *Lrat* (Figure 1H), and there was almost no contamination of other liver cell types. Furthermore, the content of retinoid, a reported HSC marker in normal liver,⁴ was significantly reduced by HFD-induced tumor progression, whereas high CD49a expression was maintained (Supplementary Figure 2, C), indicating that CD49a could be used as an HSC marker under various conditions.

The heat-stress response and related modulation in gene expression occur following enzymatic digestion at 37 °C.^{5,7} To evaluate the side effects of high-temperature enzyme incubation on transcriptome, bulk RNA-sequencing of 24346 genes of CD49a-high HSCs was performed at 37 °C or 6 °C, and the results were compared. A total of 3071 genes were overexpressed at 37 °C compared with those at 6 °C (Figure 1, I). Subsequently, pathway enrichment analysis was performed on 1144 commonly overexpressed genes. Notably, expression of several ribosomal genes, which reflects stress-mediated translation,⁸ was upregulated (Figure 1, J). We identified the top 20 co-expressed genes. The common stress responsive transcription factor *Atf3* and prototypical immediate-early response genes (*Fos* and *Jun* gene families) were overexpressed at 37 °C (Figure 1, K).

Furthermore, the enrichment analysis revealed upregulation of other stress response pathways such as ER stress signaling and inflammatory pathways under heat-stressed conditions. Nevertheless, the expression of cold shock protein-encoding genes including *Cirbp*, *Csds1*, and *Csds2* remained unchanged (Figure 1, K), suggesting that HSC isolation at 6 °C could minimize the generation of enzyme and heat-stressed transcriptional artefacts.

We applied this protocol to collect HSCs with high CD49a expression from the livers of *db/db* mice (a well-established obese model) (Supplementary Figure 3, A) and confirmed the high yield and high purity of HSCs based on *Lrat* expression. We also applied this protocol to isolate HSCs from human HCC tissue (T-hHSCs) (Supplementary Figure 3, B–C). Consistent with murine HSCs, human HSCs from HCC tissue were confirmed as a CD49a-high population among CD31⁺/CD45⁻ cells. The mRNA expression of *ACTA2* suggested that T-hHSCs predominantly consisted of activated HSCs as we observed previously^{1,2} (Supplementary Figure 3, D).

In conclusion, we developed a method to isolate HSCs from highly steatotic liver and steatohepatic HCC tissues utilizing PV-mediated enzymatic cold perfusion method to avoid heat-induced artefact gene expression. Furthermore, we identified CD49a as a reliable HSC marker under various conditions in this procedure. These results lay a foundation for investigating the role of HSCs in liver under both normal and steatotic HCC conditions.

YI CHENG*
RYOTA YAMAGISHI*
YOSHIKI NONAKA

Department of Pathophysiology
Graduate School of Medicine
Osaka Metropolitan University
(formerly Osaka City University)
Osaka, Japan

MISAKO SATO-MATSUBARA
NORIFUMI KAWADA

Department of Hepatology
Graduate School of Medicine
Osaka Metropolitan University
(formerly Osaka City University)
Osaka, Japan

NAOKO OHTANI


Department of Pathophysiology, Graduate School of Medicine, Osaka Metropolitan University (formerly Osaka City University), Osaka, Japan and AMED-CREST, Japan Agency for Medical Research and Development (AMED), Tokyo, Japan

References

1. Yoshimoto S, et al. *Nature* 2013; 499:97–101.
2. Loo TM, et al. *Cancer Discov* 2017;7:522–538.
3. Schwabe RF, et al. *J Hepatol* 2020;72:230–238.
4. Mederacke I, et al. *Nat Protoc* 2015;10:305–315.
5. O’Flanagan CH, et al. *Genome Biol* 2019;20:210.
6. Werner M, et al. *PLoS One* 2015; 10:e0138655.
7. Adam M, et al. *Development* 2017;144:3625–3632.
8. Vind AC, et al. *Nucleic Acids Res* 2020;48:10648–10661.

*Authors share co-first authorship.

Abbreviations used in this paper: HCC, hepatocellular carcinoma; HFD, high-fat diet; HSC, hepatic stellate cell; IVC, inferior vena cava; LSECs, liver sinusoidal endothelial cells; ND, normal diet; NT, non-tumor; PV, portal vein; scRNA-seq, single-cell RNA-sequencing; T, tumor; T-hHSCs, HSCs from human HCC tissue; TME, tumor microenvironment; t-SNE, t-distributed stochastic neighbor embedding.

 Most current article

© 2022 The Authors. Published by Elsevier Inc. on behalf of the AGA Institute. This is an open access article under the CC BY-NC-ND license (<http://creativecommons.org/licenses/by-nc-nd/4.0/>).

2352-345X

<https://doi.org/10.1016/j.jcmgh.2022.07.006>

Received December 29, 2021. Accepted July 11, 2022.

Correspondence

Address correspondence to: Naoko Ohtani, MD, PhD, Department of Pathophysiology, Graduate School of Medicine, Osaka Metropolitan University, Osaka, Japan. e-mail: naoko.ohtani@omu.ac.jp.

Acknowledgments

The authors thank Dr. Yoshimi Yukawa-Muto and the Department of Surgery for their help in collecting human samples used in this study. We thank Dr. Tomonori Kamiya and the laboratory members of Pathophysiology for their technical assistance. This manuscript has been edited by English editing company, Editage, which was supported by the Takeda Science Foundation.

Conflicts of interest

The authors disclose no conflicts.

Funding

This study was funded by AMED (Japan Agency for Medical Research and Development), under grant numbers JP20gm1010009 (Naoko Ohtani and Norifumi Kawada), JP20fk0210050 (Norifumi Kawada) and JP19ck0106260 (Naoko Ohtani). This study was also supported by the Japan Society for the Promotion of Science (JSPS) under grant numbers 19H04002 (Naoko Ohtani), 19H03641 (Norifumi Kawada), 21K07968 (Misako Sato-Matsubara), and 20K16309 (Ryota Yamagishi) as well as a grant from Takeda Science Foundation (Naoko Ohtani) and Yakult Bio-Science Foundation (Naoko Ohtani), and Research Grant of the Princess Takamatsu Cancer Research Fund 18-25003 (Naoko Ohtani).

Figure 1. (See previous page). Cold perfusion method for isolating HSCs minimising heat-induced artefact gene expression. CD49a is a useful HSC marker. A, The cannulation of liver via portal vein and incision of the inferior vena cava were performed in obesity-induced HCC mice (scale bars, 6 mm). The liver was perfused sequentially with EGTA, Pronase E (ProE), and collagenase. B, The histology of steatotic liver tumor in mice (hematoxylin and eosin staining, scale bar, 200 μm). In vitro enzymatic digestion and Nycodenz gradient separation. C, Flow cytometry plots for sorting CD31⁺/CD45.2⁻ cells from livers of ND- and HFD-induced HCC mice. n = 6, 35 w, (3 ND mice; 3 HCC mice). The average mouse body weight (BW): ND, 36.3 g (range, 35–38 g); HCC, 58.4 g (range, 55–61 g). D, t-SNE plots of cell clusters based on single-cell transcriptomes. E, Unsupervised clustering analysis identified HSC clusters based on *Lrat* expression. F, Unsupervised clustering analysis of *Itga1* among CD31⁺/CD45.2⁻ cells. G, Flow cytometry plots for sorting CD49a-high cells among CD31⁺/CD45.2⁻ cells from livers of HFD-induced HCC mice. n = 6, 35 w, (3 ND mice; 3 HCC mice). The average mouse body weight (BW): ND, 31.5 g (range, 30–33 g); HFD, 53.2 g (range, 45–57 g). H, Consistent unsupervised clustering analysis of *Lrat* using CD49a-high cells among CD31⁺/CD45.2⁻ cells. I, Bulk RNA-sequencing analysis of CD49a-high HSCs of ND, NT, and T tissues. n = 12, 35 w, (6 ND mice; 6 HCC mice). The average mouse body weight (BW): ND, 31.7 g (range, 28–34 g); HCC, 57.6 g (range, 51–64 g). J, Pathway enrichment analysis of the 1144 common highly expressed genes using Enrichr. K, Heatmap of the top 20 commonly overexpressed genes (above the dotted line) at 37 °C among the ND, NT, and T datasets. Heat map of the cold shock genes (below the dotted line) among the ND, NT, and T datasets.

Supplementary Methods

Mice and Diet

C57BL/6 mice (CLEA Japan) and the 2 diets (normal diet, CE2; CLEA Japan and a high-fat diet [HFD], D12492; Research Diet) were used.¹ Obese mice (>45 g; 30–40 weeks) were used in accordance with the protocols approved by the Animal Care and Use Committee of Osaka City University (Approval number: 17206). Chemically induced liver carcinogenesis was performed as described previously.¹

Isolation of Primary Hepatic Stellate Cells (HSCs)

The mice were anesthetized, and the portal vein was cannulated. After confirming the blood backflow, the catheter was connected to the perfusion line with EGTA perfusion solution (all solutions shown in [Supplementary Table 1](#) should be ice-cold). As circulation started, the inferior vena cava was cut to discard the perfused solution. The perfusion was sequentially performed using 35, 60, and 75 mL of EGTA, Pronase E (Sigma), and collagenase (Wako) solutions until the entire liver swelled up and softened ([Figure 1, A](#)). The liver was then explanted into a 10-cm dish on ice and soaked with enzyme buffer. Next, the non-tumor (NT) and tumor (T) sections were separated carefully. The NT sections turned fluid-like with pipetting, whereas the T sections remained solid and had to be minced ([Figure 1, B](#)). They were then transferred into 2 beakers with 45 mL of in vitro digestion solution and incubated for 30 minutes (6° C). The incubated tissues were filtered through a 70- μ m cell-strainer into two 50-mL tubes (NT and T), centrifuged at $600 \times g$ for 10 minutes (4° C), and the pellet was re-suspended in GBSS/B. Nycodenz (AXS) solution (0.286 g/mL) was prepared by vortexing before use. The Nycodenz gradient medium (6%–17%) was prepared, and 8 mL of cell-Nycodenz gradient medium (with the ratio shown in [Supplementary Figure 1, D](#)) was transferred into moistened 15-mL tubes and overlaid with 3 mL of

GBSS/B. The solutions were then centrifuged at $1700 \times g$ for 20 minutes (accel & brake 0; 4° C). A white intermedia layer of cells containing HSCs was obtained. A fat layer on the top was aspirated to avoid contamination. The white layer was collected and added into 40 mL of GBSS/B and subjected to low-speed centrifugation ($50 \times g$ for 5 minutes) to exclude hepatocytes. The supernatant was centrifuged at $1000 \times g$ for 10 minutes (4° C); thereafter, 3 mL of RBC lysis buffer (1 \times , Biolegend) was added to the pellet and incubated for 4 minutes to remove the erythrocytes, and then 2% fetal bovine serum (FBS)-phosphate buffered saline (PBS) was added to make up the volume to 14 mL for ceasing the reaction. Another step of high-speed centrifugation was performed at $1000 \times g$ for 10 minutes (4° C), and the pellet containing primary HSCs was re-suspended in 2% FBS-PBS solution and used for quantitative polymerase chain reaction (PCR), flowcytometry, and RNA-sequencing (RNA-seq). Although the yield of HSCs slightly varied in different mice, we could always isolate more than 10^6 cells from one ND mouse liver regardless of mouse age ([Supplementary Figure 1, F](#)) and 10×10^6 cells from the NT region and 10^6 cells from the T region of one HFD-fed mouse liver.

Quantitative PCR

Total RNA was extracted from primary HSCs using RNAiso Plus (Takara) and reverse-transcription and quantitative PCR were performed as previously described.¹ The primer sequences are listed in [Supplementary Table 1](#).

Flowcytometry and Sorting of HSCs

The isolated HSCs were pre-incubated with unlabelled anti-CD16/32 mAb (BioXcell) to avoid non-specific binding to Fc γ R. The cells were stained with antibodies against CD31, CD45.2, and CD49a (Biolegend), and analyzed using the Attune NxT Cytometer (Thermo-Fisher Scientific);

and sorted using the SONY-SH800 cell sorter (SONY). Data were processed using FlowJo-Version-10 software. Dead cells were excluded using propidium iodide (Biolegend) gating. Antibodies used are listed in [Supplementary Table 1](#).

Single-cell RNA-seq

CD31⁺/CD45.2⁻ cells from ND, NT, and T of mouse livers were sorted for single-cell RNA-seq. Single-cell dispensing and library preparation were performed according to the protocol of the ICELL8 cx 3' DE kit.² Libraries were sequenced on Illumina Novaseq 6000 with 25–150-bp paired-end reads to produce an average read of 934,102/cell. RNA-seq data of 1613 cells were obtained. The expression level of target genes in each cell was calculated using the mappa analysis pipeline (Demuxer and analyser version 1.0, ICELL8). From the gene expression matrix, quality control, data clustering, visualization, and differential expression analysis were performed using Seurat version 2.3.4 in R.³ The HSC clusters were confirmed using t-SNE of marker gene expression, including *DES* (desmin), *CYGB* (cytoglobin), and *Lrat*. CD49a-high cells among CD31⁺/CD45.2⁻ cells from ND, NT, and T tissues of mouse livers were sorted for single-cell RNA-seq (ICELL 8, Takara). The libraries were sequenced to produce an average read of 892086/cell and RNA-seq data of 1390 cells were obtained. The expression level of target genes in each cell was calculated using the Cogent NGS Analysis Pipeline.

Bulk RNA-seq

The total RNA was extracted from sorted-CD49a-high cells among CD31⁺/CD45.2⁻ cells using TRIzol (Invitrogen). Bulk RNA-seq libraries were prepared using the SMART-Seq v4 protocol (Takara). The libraries were sequenced on Illumina HiSeq4000. For each sample, depths of at least 27.6 million paired-end reads were generated. Mapping was performed using tophat. The expression level was calculated using cuffdiff and feature counts. From the gene

expression matrix, differential expression analysis was performed with R version 3.6.3.

Human Subjects

The liver tumor tissue (approximately $5 \times 5 \times 5$ mm³ tissue), obtained from a patient with HCC who underwent partial hepatectomy, was minced and stirred with enzymes for 40 minutes (6 °C), and separated following the same procedure as the murine cell isolation method. We used 20% Nycodenz gradient medium to harvest the maximum number of cells

from the limited tumor tissues. Thereafter, CD49a-high cells among CD31⁻/CD45.2⁻ cells were isolated. We isolated 7.3×10^5 HSCs labelled as T-hHSCs. The study was conducted following the Helsinki Declaration II; written informed consent was obtained from each patient according to the protocol approved by the ethics committee of Osaka City University (Approved number: 3722).

Data and Code Availability

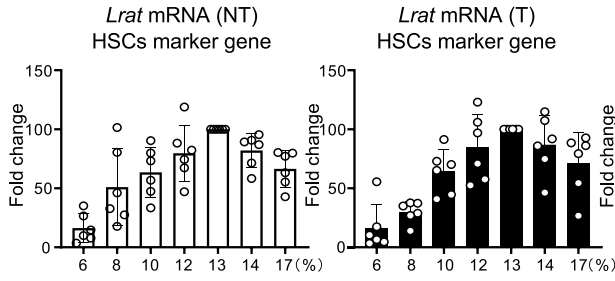
The RNA-seq data are available in the GEO databases (accession

numbers: HSCs at 37°C or 6°C: GSE192598, CD31⁻/CD45.2⁻/CD49a⁺ HSCs: GSE192582, and CD31⁻/CD45.2⁻ HSCs: GSE192637)

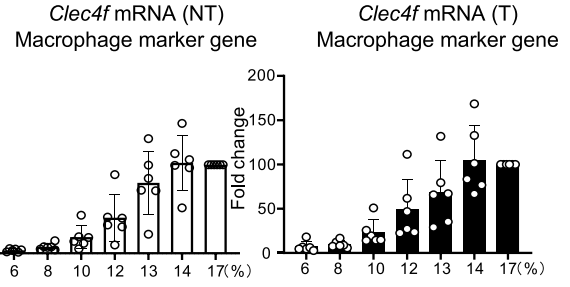
References

1. Yoshimoto S, et al. *Nature* 2013; 499:97–101.
2. Takara Bio. ICCELL8 cx 3' DE Kit User Manual. 32.
3. Butler A, et al. *Nat Biotechnol* 2018;36:411–420.

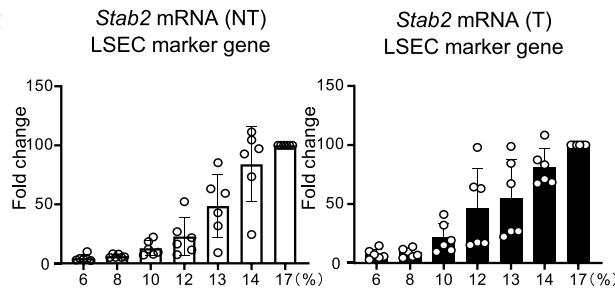
A



B



C



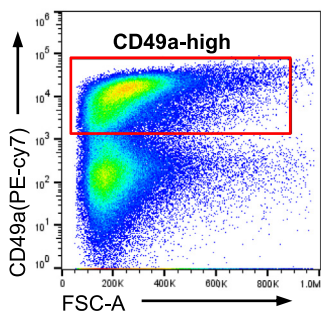
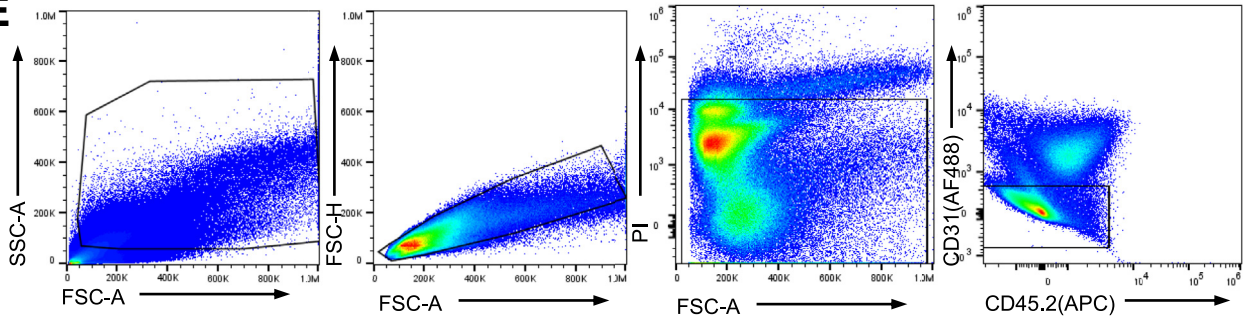
D

Nycodenz gradient medium (Nycodenz solution:cell suspension)	Nycodenz solution (ml)	cell suspension in GBSS/B (ml)
6% - (1:4)	1.6	6.4
8% - (1:2.57)	2.24	5.76
10% - (1:1.86)	2.8	5.2
12% - (1:1.44)	3.28	4.72
13% - (1:1.22)	3.6	4.4
14% - (1:1)	4	4
17% - (1:5:1)	4.8	3.2
20% - (2:3:1)	5.6	2.4

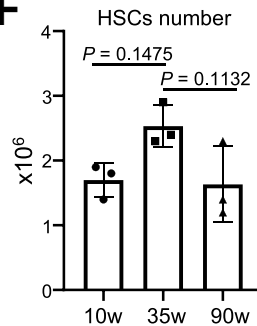
*Nycodenz solution (0.286g/ml): Nycodenz powder in GBSS/A

Rat/ GAPDH	Nycodenz	#	6%	8%	10%	12%	13%	14%	17%
			NT	#1 7.7944	27.5112	47.3347	67.2357	100	86.9493
		#2	26.5583	101.469	90.3501	82.3197	100	89.2941	79.3104
		#3	9.84728	32.814	73.2383	88.2043	100	90.629	77.0734
		#4	3.53586	17.7498	33.4454	47.0376	100	58.3121	55.2919
		#5	35.1339	80.4467	79.8536	118.81	100	71.4175	42.829
		#6	14.7123	46.1269	56.8011	74.3853	100	95.3842	63.1176
		mean	16.2637	51.0195	63.5039	79.6654	100	81.9977	66.4063
	T	#1	10.374	28.8988	65.2018	122.981	100	85.8841	88.4186
		#2	17.4179	34.9412	70.1052	70.9037	100	107.44	86.0919
		#3	3.3791	37.6	44.6156	52.4716	100	114.759	79.3364
		#4	4.60495	13.8746	40.7611	57.4921	100	46.2842	26.7422
		#5	55.5332	37.2853	91.2588	105.906	100	74.779	54.3357
		#6	6.53252	26.985	72.8805	96.9218	100	91.8666	92.7234
		mean	16.307	29.9308	64.1372	84.446	100	86.8354	71.2747
Clec4f/ GAPDH	NT	#1	1.60407	4.73271	11.262	31.9634	71.756	99.345	100
		#2	5.27147	6.66139	5.05625	9.44253	21.4703	51.3516	100
		#3	1.20675	3.8306	18.7582	39.6928	70.595	96.064	100
		#4	3.10704	7.11811	13.5389	29.8535	99.9881	105.736	100
		#5	4.72676	14.1464	43.0323	88.9705	129.466	146.752	100
		#6	3.90046	7.40401	17.8256	40.8416	84.599	112.54	100
		mean	3.30276	7.31553	18.2439	40.1107	79.4822	102.065	100
	T	#1	6.6968	12.227	19.4385	61.7416	79.3777	101.175	100
		#2	4.5867	7.49858	14.1031	27.1101	69.9966	132.686	100
		#3	4.60245	5.69413	14.5377	23.5543	35.2266	66.7578	100
		#4	6.13365	8.87888	14.7733	22.5003	28.9417	76.6885	100
		#5	18.116	16.7141	50.8896	111.503	131.781	158.466	100
		#6	2.81374	8.10603	25.5778	46.8312	65.6887	83.3284	100
		mean	7.15823	9.85312	23.22	48.8734	68.0021	104.85	100
Stab2/ GAPDH	NT	#1	3.44071	4.97695	6.99122	11.3985	42.778	111.265	100
		#2	9.90235	7.77005	7.71775	7.40495	9.03255	24.3987	100
		#3	2.4219	5.02614	12.0541	21.7908	31.7024	73.4438	100
		#4	3.55517	5.50562	9.40311	16.3404	63.1266	104.53	100
		#5	4.03833	8.07975	22.2827	52.2274	85.2317	92.6338	100
		#6	2.85766	5.03958	16.3645	26.828	59.2947	97.1001	100
		mean	4.36935	6.06635	12.8022	27.665	48.5277	83.8953	100
	T	#1	9.88627	9.71198	19.2511	63.1759	67.3006	83.2684	100
		#2	14.6218	13.8625	15.0972	17.3644	26.918	67.3275	100
		#3	5.60944	4.43002	9.43223	15.2589	26.967	68.4681	100
		#4	4.59615	5.41574	10.8573	16.9079	22.3043	71.1139	100
		#5	7.10343	11.7258	41.1108	98.0032	98.7695	108.301	100
		#6	2.93716	6.76597	32.1214	64.4611	84.4596	87.425	100
		mean	7.45904	8.652	21.3117	45.8619	54.4532	80.9839	100

E



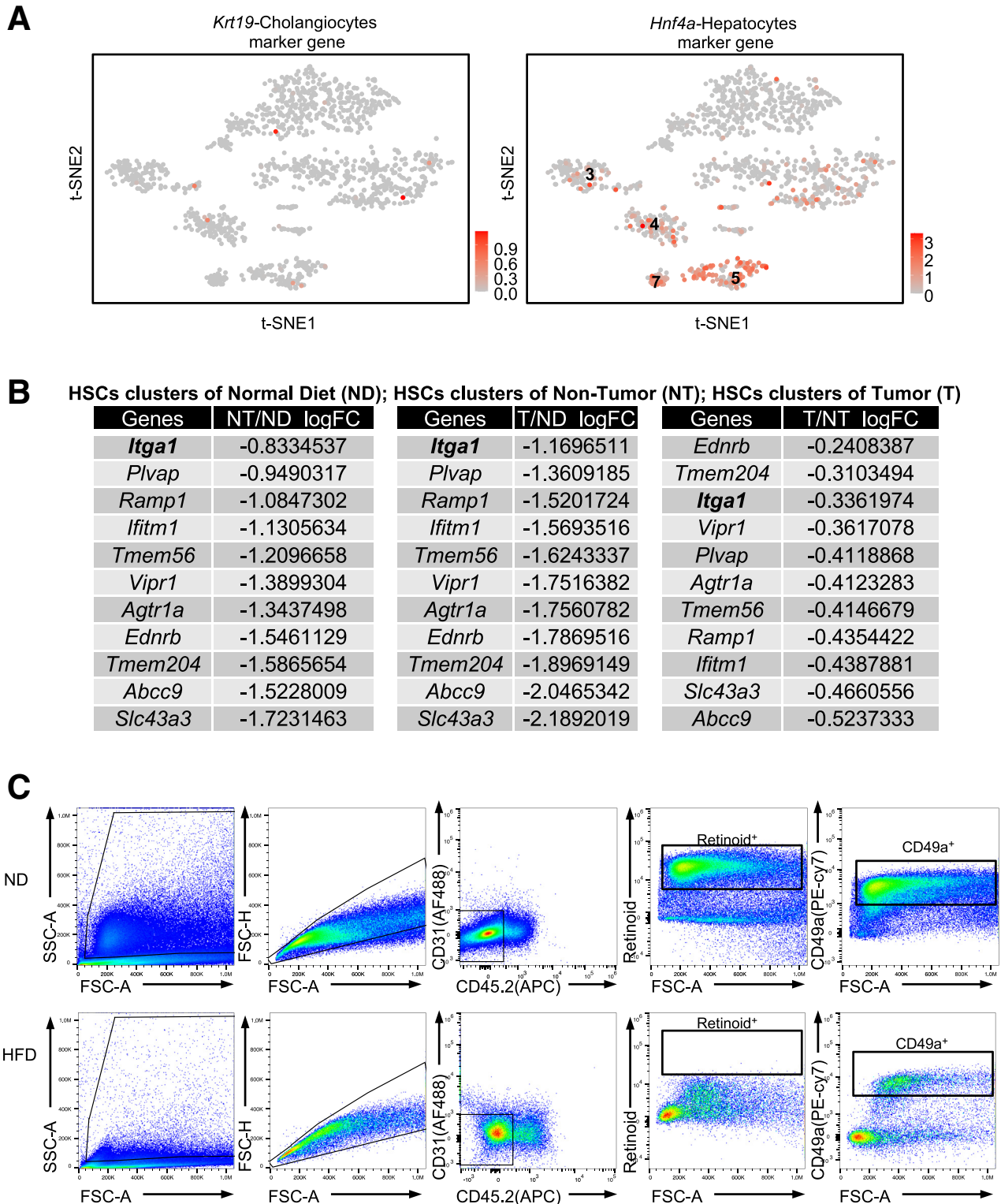
F



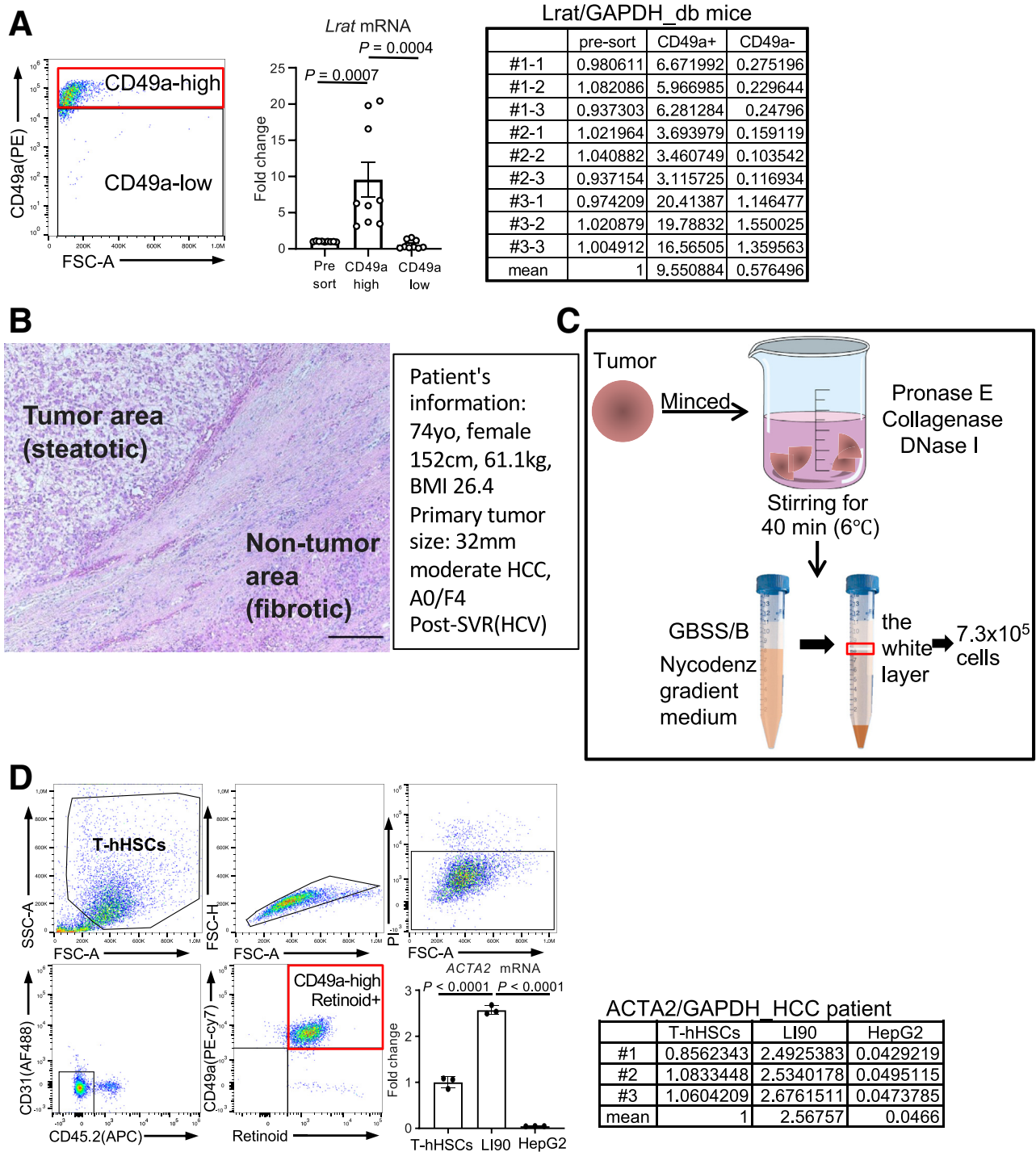
Isolated HSCs number

HSCs number (x10 ⁶) according to age			
cells number	10w	35w	90w
#1	1.8	2.9	2.3
#2	1.4	2.3	1.4
#3	1.9	2.4	1.2
mean	1.7	2.5	1.6

Supplementary Figure 1. (See previous page). Method for isolating HSCs from the livers of obese mice and mice with obesity-induced HCC. (A–C), During the Nycodenz gradient separation, 6% to 17% Nycodenz gradient medium (0.06–0.17 g/mL) was used for further experiments and purification of HSCs. The purified cells in the white layer from NT and T segments were subjected to qPCR analysis for *Lrat* (A), *Clec4f* (B), or *Stab2* (C) expression. Gene expression was normalised to *GAPDH* expression, and data are presented as fold-change difference (n = 6, 13 mice were used in 6 experiments). The average of mouse body weight was 57.6 g (range, 44–67g). The raw data are also shown in the table. (D), Nycodenz gradient medium composition. E, Flow cytometry gating strategy. F, Isolated cell number from 10-, 35-, and 90-week-old mice. The body weight of mice: 10 weeks, 25.9 g; 35 weeks, 31.5 g; 90 weeks, 30.2g. The isolated cell number is shown in the table. Statistical significance was determined using Bonferroni's multiple comparisons test (see the raw data table by the bar graph).



Supplementary Figure 2. CD49a can be a marker for HSC isolation. (A) Unsupervised t-SNE clustering of the sorted CD31⁺/CD45.2⁺ cells revealed the expression of a cholangiocyte marker (*Krt19*) and hepatocyte marker (*Hnf4a*). (B) The gene expression in the HSC clusters (ND cluster 0 and 6; NT cluster 1; T cluster 2) was compared and analyzed using log₂-Fold change (logFC). The top 11 genes encoding cell surface markers are illustrated in an ascending order of fluctuation. (C) Flow cytometry plots of HSCs from ND and HFD mice. The average body weight of mice: ND, 32.6 g (range, 31–34 g; n = 3); HFD, 58.5 g (range, 55–61 g; n = 3).



Supplementary Figure 3. CD49a-high HSCs can be isolated from the *db/db* mouse liver and the human HCC tissue. (A) Application of the cold isolation protocol for obtaining HSCs from *db/db* mice ($n = 3$). The average body weight (BW) of mice was 51.8 g (range, 48–57 g). The sorted CD49a-high and CD49a-low cells among CD31⁺/CD45⁻ cells were subjected to qPCR analysis for *Lrat* expression. Data were obtained in triplicate using the samples of 3 different mice and are presented as fold-change difference in comparison with pre-sorted HSCs. Statistical significance was determined using Bonferroni's multiple comparisons test (see the raw data table by the bar graph). (B) The histology of post-sustained virologic response (hepatitis C virus) human HCC tissue (hematoxylin and eosin staining, scale bar, 200 μ m) and the patient's information. (C) Method for isolating HSCs from T-hHSCs. (D) Flow cytometry analysis and qPCR analysis of T-hHSCs. The rectangle shows the double-positive fraction of CD49a expression and retinoid content. T-hHSCs, LI90 (human HSC line), or HepG2 (human HCC cell line) cells were subjected to qPCR analysis for evaluating *ACTA2* expression. Data were obtained in triplicate using these samples. Statistical significance was determined using Bonferroni's multiple comparisons test (see the raw data table by the bar graph).

Supplementary Table 1A. Solutions

Solutions	Reagents	Final concentration
EGTA perfusion solution	NaCl	136.89 mM
	KCl	5.37 mM
	NaH ₂ PO ₄	0.64 mM
	Na ₂ HPO ₄	0.85 mM
	HEPES	9.99 mM
	NaHCO ₃	4.17 mM
	EGTA	0.50 mM
	Glucose	5.00 mM
Enzyme buffer	NaCl	136.89 mM
	KCl	5.37 mM
	NaH ₂ PO ₄	0.64 mM
	Na ₂ HPO ₄	0.85 mM
	HEPES	9.99 mM
	NaHCO ₃	4.17 mM
	CaCl ₂ ·2H ₂ O	3.81 mM
Gey's balanced salt solution B, GBSS/B	NaCl	136.89 mM
	KCl	4.96 mM
	MgCl ₂ ·6H ₂ O	1.03 mM
	MgSO ₄ ·7H ₂ O	0.28 mM
	Na ₂ HPO ₄	0.42 mM
	KH ₂ PO ₄	0.22 mM
	Glucose	5.50 mM
	NaHCO ₃	2.70 mM
	CaCl ₂ ·2H ₂ O	1.53 mM
Gey's balanced salt solution A, GBSS/A	KCl	4.96 mM
	MgCl ₂ ·6H ₂ O	1.03 mM
	MgSO ₄ ·7H ₂ O	0.28 mM
	Na ₂ HPO ₄	0.42 mM
	KH ₂ PO ₄	0.22 mM
	Glucose	5.50 mM
	NaHCO ₃	2.70 mM
	CaCl ₂ ·2H ₂ O	1.53 mM
Pronase E perfusion solution	Pronase E in enzyme buffer	1 mg/mL
Collagenase perfusion solution	Collagenase in Enzyme buffer	1.33 mg/mL
In vitro digestion solution	Pronase E	0.556 mg/mL
	Collagenase	0.556 mg/mL
	DNase I in Enzyme buffer	0.02 mg/mL

Supplementary Table 1B. Chemicals

Reagents	Company, catalog number
Pronase E	Sigma-Aldrich, cat. no. 1.07433
Collagenase	Wako, cat. no. 032-22364
DNaseI	Roche, cat. no. 11284932001
Nycodenz AG	AXS, cat. no. 1002424
EGTA	NACALAI, cat. no. 15214-92
Sodium chloride (NaCl)	Wako, cat. no. 191-01665
Potassium chloride (KCl)	NACALAI, cat. no. 28514-75
Sodium	NACALAI, cat. no. 31720-65
di-Sodium	NACALAI, cat. no. 31726-05
HEPES	DOJINDO, cat. no. 340-01371
Sodium bicarbonate	NACALAI, cat. no. 31212-25
d-(+)-Glucose	NACALAI, cat. no. 16806-25
Calcium chloride	NACALAI, cat. no. 06731-05
Magnesium chloride	NACALAI, cat. no. 20909-55
Magnesium sulfate	NACALAI, cat. no. 21003-75
Potassium phosphate	NACALAI, cat. no. 28721-55
RBC lysis buffer (10×)	Biolegend, cat. no. 420302
D-PBS (-)	FUJIFILM, cat. no. 045-29795

Supplementary Table 1C. Equipment

Equipment	Company, catalog number
Perfusion pump	Cole-Parmer, 07516-10
Perfusion line	Cole-Parmer, 06424-14
24-gauge catheter	TERUMO SURFLO, SR-OT2419CP
70- μ m Cell strainer	AS ONE, 3-6649-02
Water bath	THERMAL ROBO, TR-1AR
Bottle-top filter, 0.45 μ m	Thermo scientific, cat. no. 291-3345
Refrigerated benchtop	Beckman Coulter, Allegra X-15R
Cell sorter	SONY-SH800, cat. no. SH800S
Attune NxT Acoustic	Thermo Fisher, cat no. A24860

Supplementary Table 1D. Primers

Gene	Primer sequences
Mouse GAPDH	5'-CAACTACATGGTCTACATGTTC-3' (forward) 5'-CACCAGTAGACTCCACGAC-3' (reverse)
Mouse <i>Lrat</i>	5'-TACTGCAGATATGGCTCTCG-3' (forward) 5'-GATGCTAATCCCAAGACAGC-3' (reverse)
Mouse <i>Clec4f</i>	5'-TGCAGGAAGCTGTGGCTGCA-3' (forward) 5'-TCCCGCCACGGCTTCTTGTC-3' (reverse)
Mouse <i>Stab2</i>	5'-ATTGCCTTAACGGGGTTCT-3' (forward) 5'-ATCGCACCAGTAACCAGGAC-3' (reverse)
Mouse albumin	5'-CCCGAAGCTTGATGGTGTGA-3' (forward) 5'-GTCTGGCTCAGACGAGCTAC-3' (reverse)
Human <i>Acta2</i>	5'-ACCTCATGAAGATCCTGACT-3' (forward) 5'-TTCAAAGTCCAGAGCTACAT-3' (reverse)
Human GAPDH	5'-GTGGTCTCCTCTGACTTCAAC-3' (forward) 5'-TGAGCTTGACAAAGTGGTCG-3' (reverse)

Supplementary Table 1E. Antibodies

Antibodies	Company, catalog number
CD16/32 mAb (2.4G2)	BioXcell, #BE0307
CD31	Biolegend, #102514
CD45.2	Biolegend, #109813
CD49a	Biolegend, #142603
Propidium iodide	Biolegend, #421301